SWELL WAVE DIRECTION OFF TWEED HEADS MONITORED BY HF OCEAN SURFACE RADAR

J.S.Bathgate, M.L.Heron and A.Prytz
[1]School of Mathematical and Physical Sciences, James Cook University, Townsville 4811, Australia.
jonathan.bathgate@jcu.edu.au

Abstract: We present results of an analysis of data collected in coastal waters off Tweed Heads during an ocean surface monitoring survey using the HF Ocean Surface Radar (COSRAD). The radar was deployed for a 30-day period during February and March of 2001 to routinely measure surface currents and wind wave parameters. The deployment also offered an opportunity to develop techniques for measuring swell wave parameters. This paper presents theory and a case study showing how second order swell peaks are observed in the Doppler spectrum. COSRAD produces an entire sweep every 30 min with spatial resolution of the order of 3 km. We average 8 adjacent pixels over a 2 h period to produce swell parameters. Swell parameters are produced from second-order (sideband) energy near the strong first-order Bragg peaks in the spectrum. Space and time averaging is done to reduce spectral noise. Our analysis indicates that the COSRAD HF radar is suitable for monitoring swell in the near-shore zone.

Keywords: HF Radar, Tweed Heads, swell waves, wind direction, Bragg scatter.

INTRODUCTION

High-frequency (HF) ocean surface radars have become well known in recent times for their ability to accurately map ocean currents over large coastal areas. Surface current measurement has been validated on numerous occasions (Prytz et al. 1999; Heron et al. 2001) since the effect was described by Crombie (1955). An advantage of systems using HF technology over traditional techniques is the area that it is capable of monitoring. Previously, surface current and wave information was restricted to directional wave buoys that measure in only one position. Although HF radar measurement of surface currents is now considered routine, the technology is still developing to allow measurement of the directional ocean wave spectrum such as wind waves and swell waves. Work by Lipa et al (1980) and, more recently, Wyatt and Holden (1994) have focussed on extracting wind wave and swell parameters from the second-order part of the Doppler radar spectrum.

The deployment of the HF COSRAD system at Tweed Heads, in south-east Queensland, was aimed to develop extraction of swell wave parameters from the long ocean wave directional spectrum. The area covered by the radar sweep included a directional wave buoy operated by the Queensland Beach Protection Authority (QBPA). This wave buoy provided a validation data set for the calculated parameters. This paper details the capabilities of the COSRAD system to monitor swell by focussing on a single day of the deployment when strong swell was observed. Methods similar to those recently used (Heron et al. 1986, Heron et al. 2002) to extract the directional wind components from HF radar are employed and a validated wind field in the coastal Tweed Heads zone is presented. Available wind speeds and wind direction data from Coolongatta Airport and the Gold Coast Seaway were used to validate these results.

CONFIGURATION OF EXPERIMENT

The purpose of this 30-day deployment of the COSRAD system was to examine swell. However, due to the versatility of this system it is also possible to routinely extract surface currents. The location of the radar was chosen to maximize its ability to carry out these objectives.

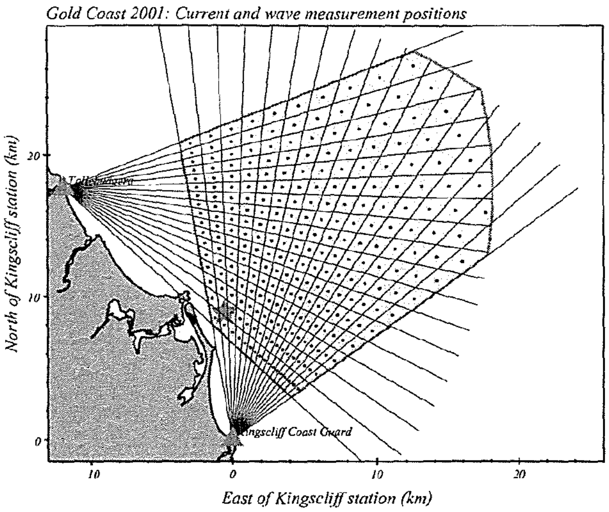

Figure 1: Configuration for the Tweed Heads deployment. The triangles mark the two stations and the asterisk marks the directional wave buoy.

Figure 1 shows two stations, located at Kingscliff (28°15.526' S, 153°34.923' E) to the south of the entrance to the Tweed River, and Tallebudgera (28°06.007' S, 153°27.661' E) to the north. These sites were selected to include a directional wave buoy run by QBPA, the probability of observing strong swell conditions in the area during this time of year and interest in sediment transportation by means of surface currents in the vicinity of the Tweed River.

HF COSRAD transmits at a frequency of 30 MHz that essentially determines the length of the resonant ocean wave, $\lambda/2$ as defined by Crombie (1955), where λ is the transmitted wavelength which is 10 m for our system. The antenna consists of an array of 8 elements, spaced half a wavelength apart – the complete array occupies an area approximately 45 m x 2.5 m. The 8 elements form a beam about 7 deg in width, which was electronically steered to 17 different angular positions. Data was collected from 12 different ranges in each of the 17 sectors, completing an entire sweep within 30 min. The azimuthal extent of coverage of each COSRAD station was approximately ±30 deg about the bore sight. The bore sights were 21 deg east of north for Kingscliff and 99 deg east of north for Tallebudgera. In order to extract reliable directional vectors for wind, surface currents and waves, it is necessary to simultaneously run two stations and for the bore sights of each station to intersect almost orthogonally.

A typical energy density spectrum collected by the COSRAD system is shown in figure 2. The two spectral lines at approximately ±0.56 Hz correspond to resonant first-order Bragg peaks. The continuum of second-order peaks surrounding these more prominent Bragg peaks are produced by a modulation of Bragg waves by longer waves in the ocean spectrum, such as wind waves and swell waves. Surface current measurements are made from the departure of these first-order peaks from this theoretical Bragg frequency.

Title:
C:\My Documents\conf_figs\sample_dopp.eps
Creator:
MATLAB, The Mathworks, Inc.
Preview:
This EPS picture was not saved
with a preview included in it.
Comment:
This EPS picture will print to a
PostScript printer, but not to
other types of printers.

Figure 2: Sample Doppler spectrum showing first-order Bragg peaks and the surrounding second-order continuum.

SUMMARY OF MEASUREMENTS

A variety of weather conditions were experienced during the deployment at Tweed Heads. As well as measurements taken using COSRAD, the wind was monitored in three locations, and the directional wave buoy provided information on wave conditions. The various sources of data are discussed separately with specific focus on 5 March 2001 (Day 22 of the deployment) to show how they compare.

Wind speed and direction records were obtained from the Kingscliff Volunteer Coast Guard logs. Their anemometer was mounted on the roof of the Kingscliff Volunteer Coast Guard observation tower at the mouth of Cudgen Creek. This was located less than 100 m from the Kingscliff COSRAD station. Other records were obtained from anemometers located at Coolangatta Airport (28.17° S, 153.50° E) and the Gold Coast Seaway (27.94° S, 153.43° E). The deployment began with relatively calm wind conditions that rarely exceeded wind speeds of 5 ms^{-1}. Much stronger wind conditions were observed on two occasions, between day 5 to

Title:
C:\My Documents\conf_figs\cool_wnd_speeds.eps
Creator:
MATLAB, The Mathworks, Inc.
Preview:
This EPS picture was not saved
with a preview included in it.
Comment:
This EPS picture will print to a
PostScript printer, but not to
other types of printers.

Figure 3: Variation in wind speeds during the COSRAD deployment. Measurements taken from Coolongatta Airport.

10 of the deployment and again from day 20 to 25. During these periods wind speeds reached up to 13 ms^{-1} and are generally in excess of 10 ms^{-1}. These 'events' can be seen in the wind records from Coolangatta airport and plotted in Figure 3.

Directional information adds to the understanding of these conditions and we are able to distinguish between the two distinct strong wind periods and the background weaker periods. Figures 4(a) and (b) display the easterly and northerly components of the wind speeds respectively. It is easy to see that the periods of weaker wind, less than 5 ms^{-1}, correspond to a diurnal variation in wind conditions, such as on-shore sea breezes. The stronger wind periods noted in figure 3 are matched by periods of strong northerly components of wind speed as shown in figure 4(b). This corresponds to a synoptic scale weather system.

Title:
C:\My Documents\conf_figs\est_comp_cool_wnd.eps
Creator:
MATLAB, The Mathworks, Inc
Preview:
This EPS picture was not saved
with a preview included in it
Comment:
This EPS picture will print to a
PostScript printer, but not to
other types of printers

Title:
C:\My Documents\conf_figs\nth_comp_cool_wnd.eps
Creator:
MATLAB, The Mathworks, Inc
Preview:
This EPS picture was not saved
with a preview included in it
Comment:
This EPS picture will print to a
PostScript printer, but not to
other types of printers

Figure 4: Coolangatta Airport (a) Easterly component of wind speed, (b) Displays the Northerly component of wind speed.

The directional variation of wind waves from the QBPA wave buoy supports this. Figure 5 shows the direction of propagation of wind waves throughout the deployment. Day 22 is marked to show the wave direction at the time of the strong wind in the northerly direction.

Title:
C:\My Documents\conf_figs\wnd_wav_22.eps
Creator:
MATLAB, The Mathworks, Inc.
Preview:
This EPS picture was not saved
with a preview included in it.
Comment:
This EPS picture will print to a
PostScript printer, but not to
other types of printers.

Figure 5: Directional variation of wind waves from the QBPA wave buoy. The dashed line marks day 22 of the deployment.

All data on 5 March 2001 indicate the wind direction as southerly (ie blowing towards the north). Extraction of wind directions from HF radar is common and involves calculating the ratios of the two first-order Bragg peaks. In the relationship,

$$\phi = \left| 2\arctan(R^{1/2S}) \right| \qquad (1)$$

R is the power ratio of the Bragg peaks, S is a spreading parameter and ϕ is the direction of wind with respect to the beam direction. However, there is an inherent ambiguity in this calculation as to which side of the beam this angle belongs. Using both COSRAD stations resolves the ambiguity. At each point in a radar sweep wind directions $\pm\phi$ would be calculated for each station. In this way the relative directions can be compared between stations and the ambiguity resolved. The stick plot of wind directions shown in Figure 6 is an average of the wind field over a period of 2 h, between 1000 and 1200 h, on the 5 March 2001. The wind is dominantly blowing towards the north, which compares very well with the data from the wave buoy (Figure 5) and the Coolangatta Airport anemometer (Figure 4).

Title:
C:\My Documents\conf_figs\ave_wind5thmar.eps
Creator:
MATLAB, The Mathworks, Inc.
Preview:
This EPS picture was not saved
with a preview included in it.
Comment:
This EPS picture will print to a
PostScript printer, but not to
other types of printers.

Figure 6: Average wind field as measured by COSRAD between 1000 h and 1200 h on the 5 March 2001. A nominal value S=2 was used here.

Surface currents observed for the duration of the deployment can be divided into two distinct phases. For the majority of the time, from the beginning of the deployment through to day 18, the surface currents were dominated by a strong southwards flow. Even during periods of strong winds from the south the currents remained dominantly southwards, although they were somewhat more complex. The second period coincides with the stronger of the two wind periods discussed above, day 19 to day 23. This saw some occasions where surface currents across the entire area were flowing northwards. Figure 7 shows the state of the surface currents on day 22 of the deployment when the wind was blowing strongly from the south.

FREQUENCY MODULATION OF THE RADAR ECHO

The dominant scattering mechanism for ocean radar backscatter is Bragg scattering from the surface wave which is propagating towards (or away from) the radar with a wavelength half the radar wavelength. For the HF COSRAD system, the operating frequency is 30 MHz and the Bragg wavelength is 5 m. When there is an underlying swell, the Bragg waves are thrust

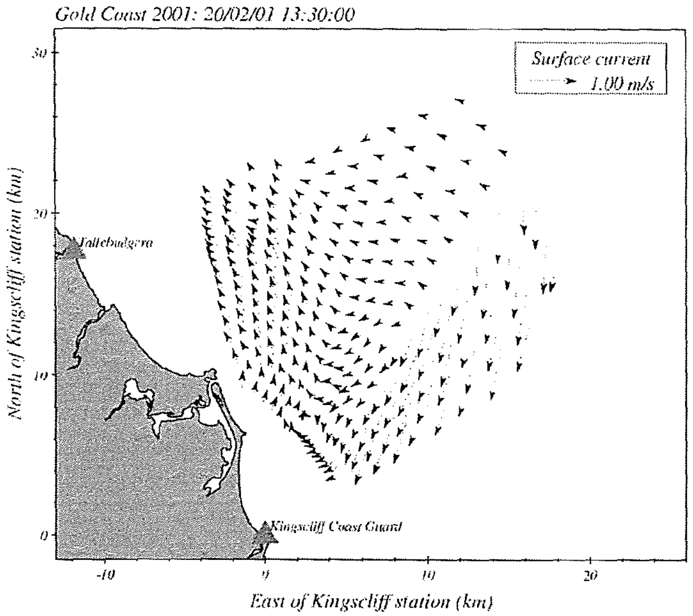

Figure 7. Surface currents as measured by COSRAD under strong southerly wind conditions.

to and fro by the faster moving long wavelength swell so that at any given point on the surface the velocity of the Bragg wave is determined by the propagation of that wave, and by the surge velocity imposed by the swell. We assume that these velocities are linearly superposed. The instantaneous surge velocity of a parcel of water at the surface is

$$v_S = a_S \omega_S \tag{2}$$

where a_s is the amplitude of the swell wave, and ω_S is the frequency, and the trajectory of the surface parcel is a circle in the vertical plane. The horizontal component of the surge velocity is

$$v_{SH} = a_S \omega_S \cos(\omega_S t) \tag{3}$$

If we wish to consider the swell surge velocity in a direction θ from the direction of propagation of the swell, then it is a simple projection and the horizontal component is given by

$$v_{SH} = a_S \omega_S \cos\theta \cos(\omega_S t) \tag{4}$$

This velocity modulates the phase velocity of the Bragg wave and produces a frequency modulation on the Doppler shifted backscatter echo. The resulting spectrum is a series of Bessel functions when the modulating function is a monotonic sinusoid, as used here. For a small modulation index the spectrum is dominated by the carrier, (the first-order Bragg line) and the first pair of side lobes, with a minor contribution from the higher order sidebands. We can calculate the spectral amplitudes for any set of two-scale parameters. Figure 8 shows calculated spectra for the conditions of a case study on 5 March 2001 when there were strong winds from the south.

From the radar spectra the estimate of the ratio (R_{swell}) of first-order Bragg amplitude to the mean amplitude of the first sidebands is simple and is a reliable and robust parameter to extract. R_{swell} is a minimum when the radar beam points in the direction of the swell ($\theta = 0$) and is infinite when the beam points orthogonal to the swell direction and receives no modulation from the surge velocity of the swell. In the next section we investigate the variation of R_{swell} versus θ by comparing the two-scale analysis with data from the radar deployment at the Gold Coast.

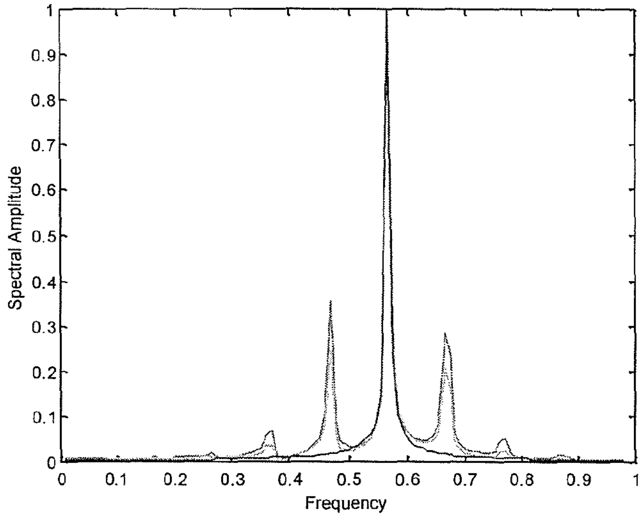

Figure 8. Spectra from the two-scale model. $\theta = 0$ gives the highest sidebands. The other sidebands are for $\theta = 45°$ and 90°. The amplitudes fit the case study on 05/03/2001.

In figure 9 calculated swell peak power ratios are plotted against the radar beam direction. The relative power ratio was scaled according to the swell amplitude and the horizontal axis according to the swell direction. In this case the radar sweep has captured the minimum portion of the modulation. From figure 9 the swell direction is estimated to be 112 deg. More accurate swell directions could be obtained if the radar sweep happened to cover the peak rather than the minimum, simply due to the slight inaccuracies in determining the exact position of a shallow minimum. The fitted modulation from this analysis describes the radar ratios well across the 60 deg extent of the sweep.

All the analysis shown here allows for monochromatic, unidirectional swell. For complex swell situations, such as bimodal swells, the analysis above may be inadequate. Our analysis requires the swell peaks to be distinct and separate. In situations such as bimodal swells the peaks are likely to merge making our analysis unable to distinguish between them.

CONCLUSIONS

It has been shown that dominant swell direction can be extracted from HF radar using a frequency modulation technique. This adds to the COSRAD system's capabilities of describing the near-shore zone. Adding extraction of swell parameters to routinely mapped surface current vectors and wind directions improves the versatility of the system. The experimental configuration for the purpose of swell extraction was not optimal in this case.

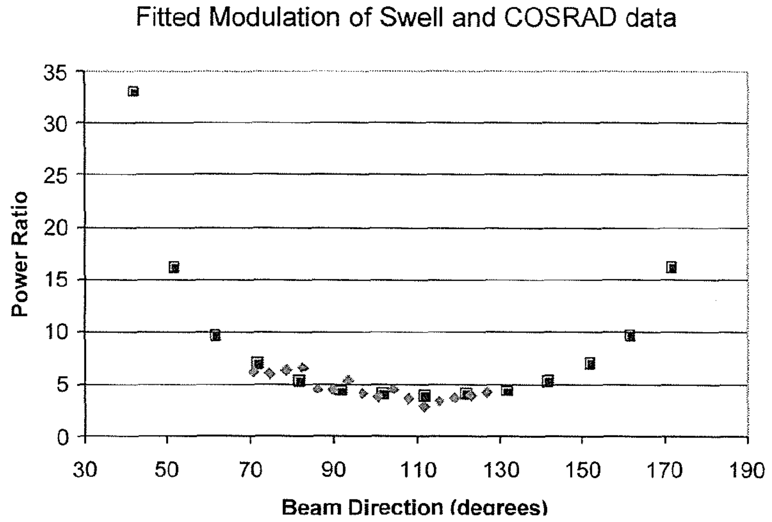

Figure 9: Graph of the power ratio of swell peaks from COSRAD (diamonds) and the fitted swell modulation data (squares).

However, configurations for future deployments can be altered to improve this. Aligning the two stations differently so that they cover a combined 120 deg would ensure that the cusp of modulation is covered. This would improve the accuracy of swell direction estimates and developments into swell period and height could be examined.

ACKNOWLEDGEMENTS

We are grateful to the Gold Coast City Council, and the Queensland Environmental Protection Agency for approvals and access to the Tallebudgera site; and to the Tweed Shire Council for approvals and access at Kingscliff. We appreciate willing assistance from Paul Vasey and access to power from the Tallebudgera Outdoor Recreation Centre. A very special thanks is due to Ted Griffiths, Commodore of the Kingscliff Volunteer Coastguard, for access to power, and wind observations, and also for his wealth of general local knowledge.

REFERENCES

Crombie, D.D., 1955. Doppler spectrum of sea echo at 13.56Mc/s, *Nature, 175:* 681-682.

Heron, M.L., and Rose, R.J. 1986. On the application of HF ocean radar to the observation of temporal and spatial changes in wind direction. *IEEE Journal of Oceanic Engineering, OE-11:* 210-218.

Heron, M.L, Prytz, A. and Bathgate, J.S. 2001. Currents off Tweed Heads by HF ocean surface radar, Coastal and Ocean Eng. Conf., IEAust., 49-54.

Heron, M.L and Prytz, A. 2002. Wave height and wind direction from the HF coastal ocean surface radar, *Can. J. Remote Sensing, 28:* 385-393.

Lipa. B, and Barrick, D. 1980. Methods for the extraction of long-period ocean wave parameters from narrow beam HF radar sea echo, *Radio Science, 15:* 843-853.

Prytz, A. and Heron, M.L. 1999. On the flushing of Port Phillip Bay: an application of HF ocean radar, *Mar. Freshwater Res., 50:* 483-492.

Wyatt, L.R. and Holden, G.J. 1994. HF radar measurement of multi-modal directional wave spectra, *Global Atmos. Ocean Sys., 2:* 265-290.

Keywords: HF Radar, Tweed Heads, swell waves, wind direction, Bragg scatter.